INCREASING SCANNING RANGE OF MEMS MIRRORS FOR ENDOSCOPIC OPTICAL SYSTEMS VIA SUBMERSION IN HIGH RI FLUIDS

Kevin Zhu, Huikai Xie Ph.D.[1], and Liang Zhou Ph. D.[1]

[1]Department of Electrical & Computer Engineering, University of Florida, Gainesville, FL, USA

***Abstract*—MEMS (microelectromechanical systems) scanning mirrors are used extensively in laser scanning microscopy and medical endoscopic optical systems due to their small size, low per-unit cost, and efficient power consumption. However, due to the fragility of MEMS actuator systems, their scanning range is often severely compromised, reducing their efficacy in imaging applications. Using the Snell's window phenomenon, this issue can be rectified by submerging the mirror into a fluid with a high RI (refractive index). In order to test the effectiveness of these submersion fluids, a copper/tungsten bimorph MEMS mirror, whose central plate measured 550*550 µm, was submerged in ethyl cinnamate, mineral oil, and silicone oil (with refractive indices of 1.56, 1.45, and 1.39 respectively) and an increase in the mirror's maximum output angle was observed. Further optical tests revealed that the submersion fluids distorted the laser beam, changing the laser spot both in size and in shape. Additionally, as a result of the fluids' high viscosity and dampening effects, the submerged MEMS mirror could not perform resonant scanning, and its maximum actuation frequency was limited to 100 Hz. Further experimentation to solve the distortion and response time issues in submerged MEMS mirror systems will be required; alternative high RI submersion fluids also need to be tested. Nevertheless, this submersion technique has the potential to be a very successful yet simple way of producing a wide-angle scanning device, which could open greater opportunities in optical systems using MEMS mirrors.**

Keywords—MEMS mirror, electrothermal actuator, output angle, mechanical tilting, submersion fluid, refractive index, Snell's law, viscosity, thermal conductivity, mineral oil, silicone oil, ethyl cinnamate

I. INTRODUCTION

MEMS (microelectromechanical systems) technology is ubiquitous in today's society; it is used extensively in scientific research and is also the reason why many devices today, such as smartphones, digital cameras, and projectors, are feasible [1]. The MEMS scanning mirror is a specific type of MEMS technology that is used in the fields of medical and scientific imaging. It is a highly miniaturized version of the traditional scanning mirror, which utilizes electric motors to tilt a reflective pane that directs the path of a laser beam. This scanning method is used in fluorescence microscopy and OCT (optical coherence tomography), where the laser beam is steered to scan the specimen, and output signals – fluorescence or interference – are collected to produce an image [2].

Conventional setups use large and very powerful lasers with bulky scanning mirrors; their size makes examining specimen such as live animals incredibly difficult, limiting the research potential of these devices [3]. In order to enhance their functionality, scanning systems can be miniaturized with the use of MEMS mirrors, whose reflective panes often measure in the micrometer scale.

Traditional electric motors cannot move such minute mirrors. Instead, MEMS mirrors use various actuation systems based on the electrothermal, electrostatic, electromagnetic, and piezoelectric properties of certain materials [4]. Electrothermal bimetal actuators have been developed to produce an actuation system that achieves large scan angles at lower driving voltages. They work based on the differences in coefficients of thermal expansion of certain metals; when heat is applied, some materials expand more readily than others. In these actuators, metals that have very different coefficients of thermal expansion are placed into a bimetal structure. When a current runs through the bimorph, the resistance of the metals generates heat, causing the entire structure to bend and flex. The experiment used an inverse series copper/tungsten bimorph actuation system that generates large vertical displacement while cancelling tip-tilt and lateral shift. The copper/tungsten bimorphs also have vastly different coefficients of thermal expansion and relatively high Young's Modulus. This allows for the creation of electrothermal actuators that are more robust, thinner, and more responsive than other bimorph structures [5].

Despite MEMS mirrors' many advantages – such as their small size, efficient power consumption, and relatively low per-unit cost – they still suffer from a fundamental mechanical limitation: their size. The tiny actuators used to move them are fragile, which greatly reduces the scanning range of many MEMS-based devices. In order to solve this issue without altering their mechanical design, MEMS mirrors can be submerged in a fluid with a high RI (refractive index) to take advantage of the Snell's window phenomenon. This works because Snell's law dictates the degree that a light beam changes trajectory once it moves into a different medium ($n_1 * \sin\theta_1 = n_2 * \sin\theta_2$, where n_1 and n_2 are the refractive indices of medium 1 and medium 2 respectively; θ_1 is the angle of incidence and θ_2 is the angle of refraction).

As depicted in Fig 1, the reflected light from the submerged MEMS mirror is further deflected once it crosses the fluid-air boundary. This artificially enlarges the scanning range of the device by a factor of the fluid's RI value without needing to physically increase the mechanical tilt angle of the mirror itself [6].

Previous attempts of this method used mineral oil as the submersion fluid due to its low cost, chemical stability, relatively high refractive index (1.45), and low vapor pressure. Despite those advantages, there are many other liquids with much higher RI values that could be candidates for submersion fluids. As such, the main goal of this experiment is to find a liquid with a higher RI value than mineral oil that could still facilitate the function of a MEMS mirror.

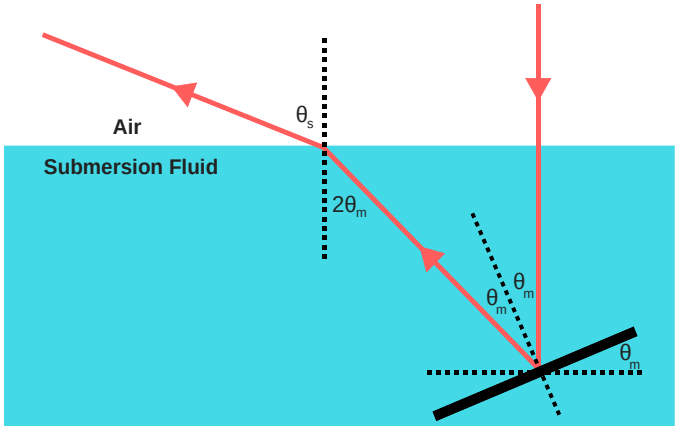

Fig. 1 *Device concept: θ_s is the final output angle of the MEMS mirror and is affected by the refractive index of the submersion fluid.*

There are many liquids with refractive indices greater than that of mineral oil. However, other properties of the submersion fluid – such as toxicity, vapor pressure, thermal and electrical conductivity, viscosity, and corrosiveness – could affect the performance of the MEMS mirror. With these considerations, non-aqueous solutions are prime submersion fluid candidates, as they have lower vapor pressures, are not electrically conductive, and have high RI values. However, most oil-based liquids are rather viscous and any submersion fluid could alter the dispersion of the laser beam [7]; further tests are needed to see if the MEMS mirror's response time, scanning speed, and power consumption are compromised.

MEMS scanning mirrors' small size, lower power consumption, and economic cost are very advantageous in the field of medical and scientific imaging. Thus, finding a submersion fluid that dramatically improves their scanning range would give MEMS mirror technology much broader applications, which could lead to even greater research advancements in the future.

II. Methods

A. MEMS mirror bonding and testing

The MEMS mirror as shown in Fig 2 was provided by WiOptix Inc. After the mirror's fabrication, it needed to be gold-wire bonded to a DIL (dual-in-line) platform.

The package was attached to a breadboard and examined with a microscope to pair each of the four actuators to its corresponding wire, making it possible to fine-tune the mirror's movements.

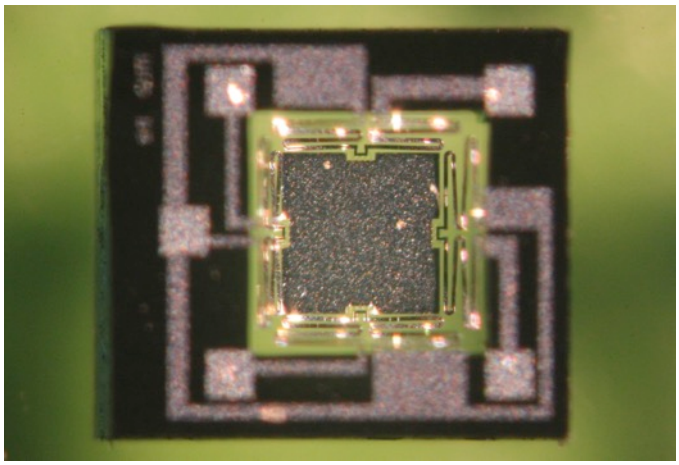

Fig. 2 *MEMS Scanning Mirror provided by WOI. Mirror plate measures 550*550 μm.*

To prep the MEMS mirror for the experiment, the DIL frame was removed from the breadboard. This was necessary because the circuit board would have soaked up all the added liquid, damaging it and preventing the MEMS mirror from actuating. The eight pins on the package were removed and five wires (four actuator wires and one ground wire) were soldered onto the frame. As shown in Fig 3, this entire set up was then glued on top of a glass pane. With the MEMS mirror oriented vertically, it was placed into a petri dish that was later used to hold the high RI fluids. The glass pane was not permanently attached to the petri dish; the MEMS mirror could be easily removed and cleaned when swapping fluids.

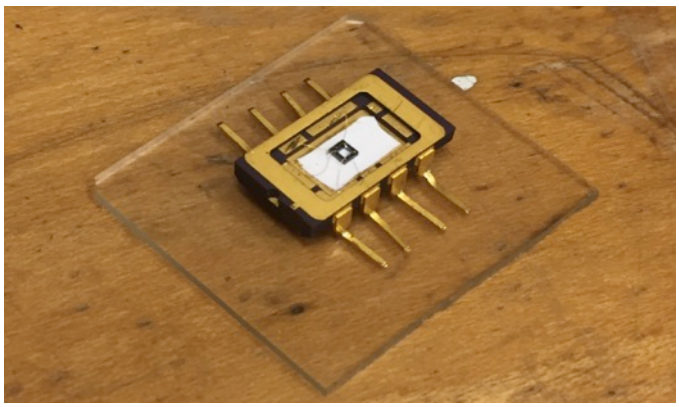

Fig. 3 *MEMS mirror gold-wire bonded to DIL package and glued onto glass pane*

B. Experimental setup

The MEMS mirror setup was also mounted onto a 2-axis stage, which was all attached to a magnetic base. A 680 nm 10mW helium-neon laser was mounted onto a 2-axis stage and oriented above the MEMS mirror setup with its beam pointed down perpendicularly to the mirror's surface.

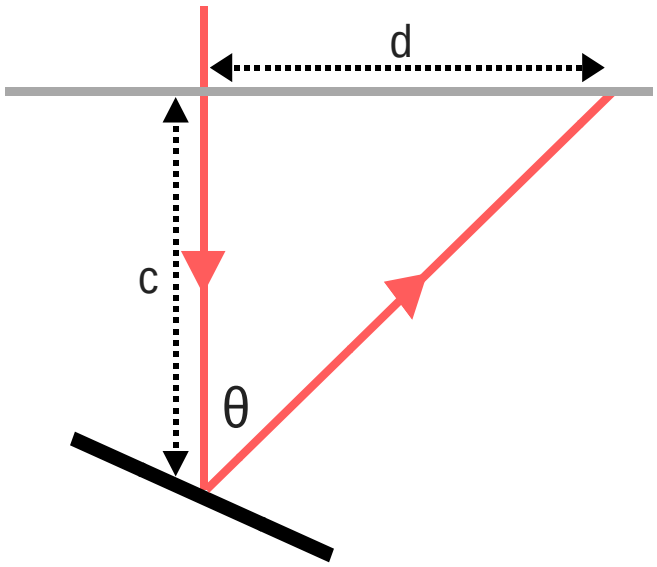

Fig. 4 *Length c (distance between graph paper and MEMS mirror) and length d (displacement value of laser spot) used to calculate θ (output angle).*

A piece of graph paper was attached onto a glass pane and placed directly below the laser. A pinhole was made on the graph paper so that the laser beam could pass through it unimpeded and reflect off of the MEMS mirror. As depicted in Fig 4, the final output angle of the mirror was calculated by measuring the distance between the pinhole and the laser spot projected onto the grid.

The graph paper's grid measured in 2.5 mm increments vertically and 2 mm increments horizontally, as shown in Fig 5(b). By driving different actuators, more displacement values could be measured accurately, thereby increasing the resolution of the results.

C. Experimental setup calibration

The laser beam needed to be oriented perpendicularly to the fluid's surface, the mirrors' surface, and the graph paper. Due to the nature of liquids, the orientation of the submersion fluid's surface was always constant and thus used as the leveling point of the experiment. As shown in Fig 4(c), the 2-axis stage attached to the laser helped orient the laser beam perpendicularly to the fluid's surface.

The MEMS device was placed directly underneath the setup so that the mirror pane reflected the laser beam. Its lateral position was subsequently locked using the magnetic base. With the 2-axis stage, the mirror's orientation could then be fine-tuned to be perpendicular to the laser beam; the fluid's surface was always level and thus its alignment never changed even when the mirror's stage was operated. Finally, the glass sheet with attached graph paper was mounted between the laser and the mirror, and its orientation was adjusted to be perpendicular to the laser beam.

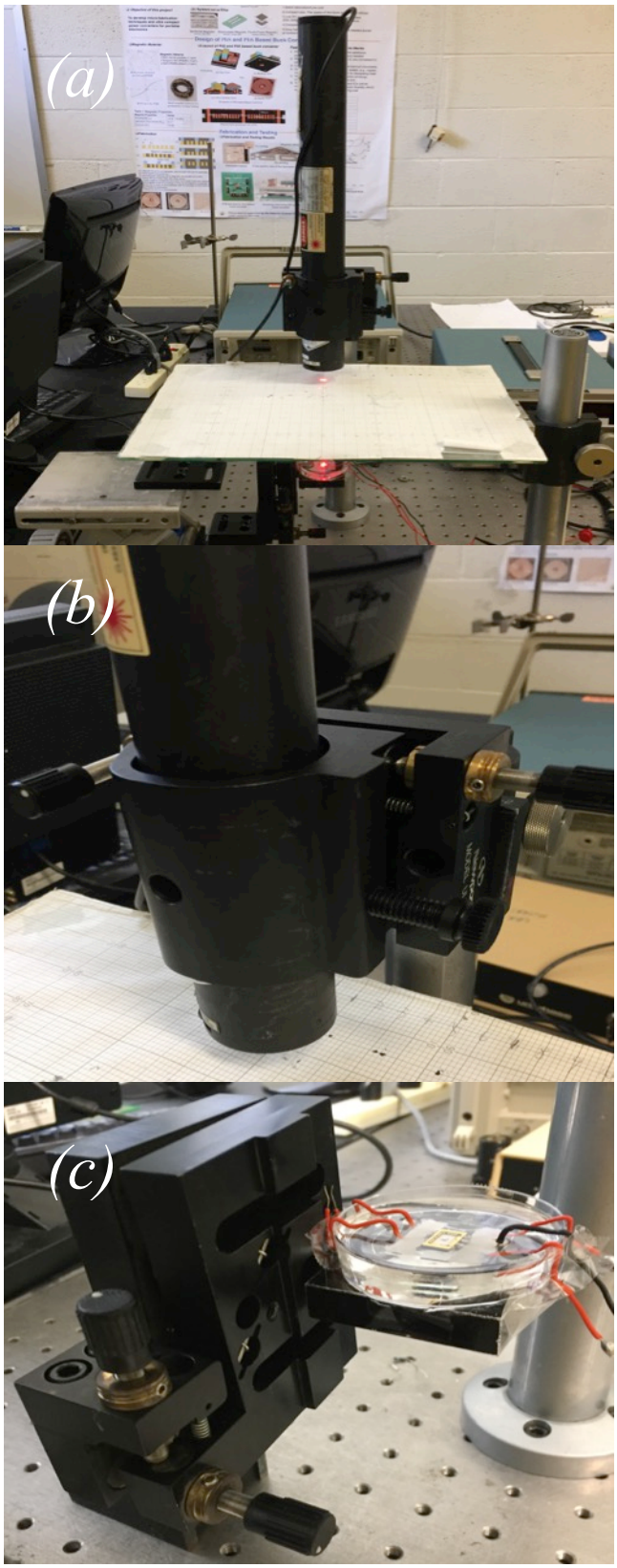

Fig. 5 *(a) Overall setup of experiment. (b) 2-axis stage used to orient mirror perpendicularly to laser beam. Magnetic base used to adjust and lock mirror's lateral position. Petri dish contains high RI fluid and MEMS mirror. (c) 2-axis stage used to fine-tune laser's orientation. Individual squares on graph paper measured 2 by 2.5 mm. Pinhole was made on the graph paper to facilitate output angle calculations.*

D. *Input voltage and static output angle data collection:*

In order to test and compare the MEMS mirror's power consumption and maximum static output angle across different submersion fluids, input DC voltage was slowly applied to the electrothermal actuators so that the displacement values increased in either 2 mm or 2.5 mm increments (depending on which actuator was driven) before stopping at the mirror's voltage and mechanical tilt limit.

Each displacement value's corresponding voltage was recorded with a voltmeter, and the results were used to examine the effects of each submersion fluid on the MEMS mirror's performance – such as driving voltage requirements and maximum static output angle.

E. *Laser spot size measurements*

Possible light distortion caused by the refractive indices of the submersion fluids would have detrimental effects on the clarity of images produced by submerged MEMS mirror optical systems.

To account for this potential issue in later research, DC voltage was applied to the MEMS mirror's actuators and the diameter of the projected laser spot on the graph paper was measured using the grid and calipers at incremental displacement values (which were subsequently converted into equivalent output angles). These measurements were repeated for each submersion fluid to observe the optical interference induced by a liquid environment.

Visual changes in the laser spot's shape as well as any variations in laser beam's optical quality were also noted.

F. *Dynamic Frequency Testing*

Performance changes were expected to occur when the MEMS mirror was submerged into a more viscous environment; AC voltage was applied to the MEMS mirror's electrothermal actuators to observe the submersion fluids' dampening effects on the mirror's ability to performing rapid scanning.

When AC voltage is applied, MEMS mirrors will tilt back and forth, tracing out a path with the laser beam. By measuring the length of the path using calipers, the scanning angle of the MEMS mirror can be calculated. As such, the input frequency of the AC power supply was increased incrementally and each corresponding output scan angle from the mirror was recorded (as shown in Fig 6).

Along with the size of their scanning range during high frequency testing, the submerged MEMS mirror was also tested to see if it could perform resonant scanning.

III. Results

A. *Input voltage and static output angle results*

As shown in Fig 6, the maximum static output angle of the MEMS mirror was recorded to be ±13° at 6V in open air, ±18.3° at 13V in silicone oil, ±19.1° at 13V in mineral oil, and ±20.4° at 10V in ethyl cinnamate. At voltages below 6V, the MEMS mirror's output angle in open air was almost double that of the submersion fluids.

However, as the voltage increased to 10V, the output angle of the mirror submerged in silicone oil and mineral oil eventually surpassed the maximum scanning angle of the mirror in open air. When the voltage increased to 8V, the output angle of the mirror submerged in ethyl cinnamate surpassed the maximum scanning angle of the mirror in open air.

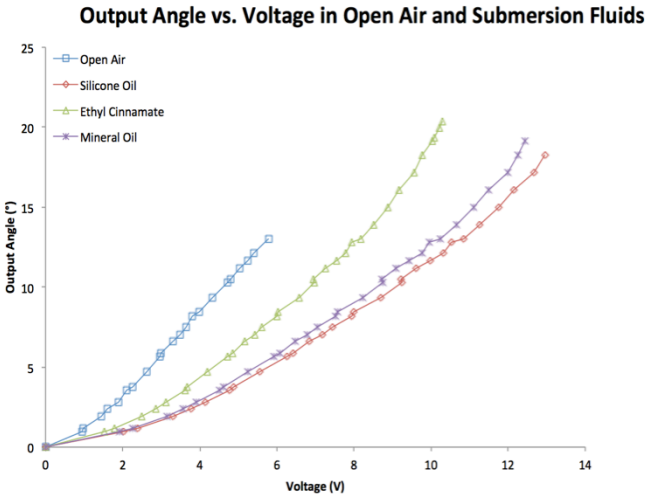

Fig. 6 *Static output angle vs. voltage in open air, silicone oil, ethyl cinnamate, and mineral oil. Power curves and maximum output angles recorded.*

As depicted in Fig 6, there was a positive linear relationship between driving voltage and the mirror's output angle in open air. In contrast, during submerged MEMS mirror testing, the output angle increased more rapidly at higher voltages.

The voltage was stopped at 6V for open-air angle testing, 13V for silicone oil and mineral oil angle testing, and 10V for ethyl cinnamate due to the mechanical failure of the actuators under high temperature generated by the driving voltage.

B. *Optical measurement results*

The spot size was constant for all output angles in open air testing. When DC voltage was applied to the MEMS mirror actuators while the device was submerged, the resulting spot size from the reflected laser beam expanded as the output angle increased.

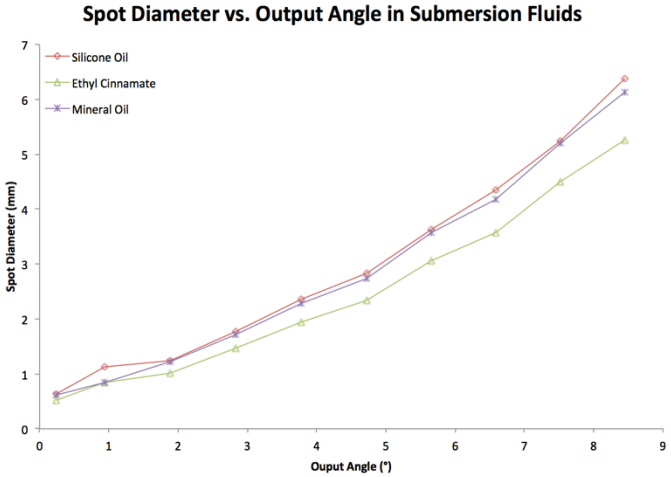

Fig. 7 *Results from spot size measurements for silicone oil, ethyl cinnamate, and mineral oil.*

As shown in Fig 7, the laser spot diameter grew from 0.5 mm to 6.4 mm in silicone oil, 6.1mm in mineral oil, and 5.2 mm in ethyl cinnamate as the output angle was increased to 8.44°. Due to the distortion effects of the fluids, the laser spot's shape was also altered considerably, making it more oblong shaped than circular during submerged testing. As a result, diameter measurements close to the MEMS mirror's mechanical tilting limit were rather inaccurate.

C. Dynamic Testing Results

For dynamic testing, the amplitude and offset voltage for open air testing was 2.2V and 3V respectively (input voltage ranged from 1.9V to 4.1V). As shown in Fig 8(a), the output angle diminished from 3.8° to 1.32° across the frequency range from 0.1 Hz to 1500 Hz. At 1422 Hz, the MEMS mirror reached its resonance frequency and the output angle spiked to 5.4°.

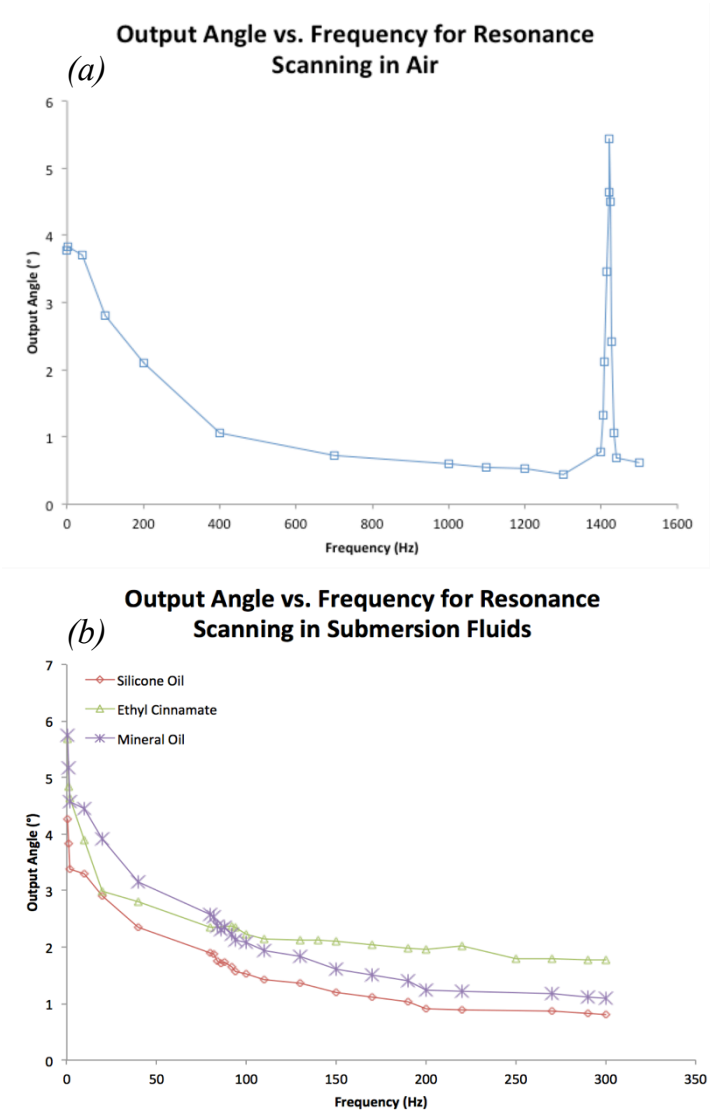

Fig. 8 *Dynamic frequency and resonance testing in (a) open air (resonance occurs at 1422 Hz) and (b) submersion fluids (silicone oil, ethyl cinnamate, and mineral oil).*

The amplitude used for the silicone oil testing was 6V and the offset voltage was 6V (input voltage ranged from 3V to 9V). The amplitude used for the ethyl cinnamate testing was 3V and the offset voltage was 2.6V (input voltage ranged from 1.7V to 4.3V). The amplitude used for the mineral oil testing was 6V and the offset voltage was 6V (input voltage ranged from 3V to 9V).

As shown in Fig 8(b), the output angles during submerged MEMS mirror testing diminished from 4.3° to 0.8°, 5.7° to 1.8°, and 5.7° to 1.1° across the frequency range from 0.1 Hz to 300 Hz for silicone oil, ethyl cinnamate, and mineral oil respectively. The MEMS mirror never reached resonance frequency when it was submerged in fluid.

IV. Discussion

A. Input voltage and static angle analysis

The primary purpose of the experiment was to increase the MEMS mirror's scanning range by submerging it into a high RI fluid. As such, output angle vs. voltage results were compiled and compared to observe driving voltage efficiency and maximum output angles in each submersion fluid.

In open air, there was a linear relationship between the output angles of the MEMS mirror and the corresponding driving input voltages. However, during submerged MEMS mirror testing, the fluid environment surrounding the mirror was far more thermally conductive than air. As shown in Fig 6, this prevented the electrothermal actuators from heating up adequately and impeded the mirror's movement, thereby reducing the output angle for the same input voltage. Along with the higher thermal conductivity of the fluid, the MEMS mirror's more restrictive environment exacerbated the issue, which meant an increased amount of voltage was needed to obtain similar output angles.

The silicone oil and mineral oil submersion fluids were rather viscous and thermally conductive [8], therefore higher voltages were needed to reach the failure point of the electrothermal actuators and the MEMS mirror's mechanical tilting limit. However, once higher voltages were applied, enough physical tilting occurred for the mirror to take advantage of Snell's law; at the edge of the mirror's actuation limit, the output angle increased much faster as more voltage was applied. Despite the scanning range improvement (showcased in Fig 6: ±13.0° in open air to ±18.3° in silicone oil and ±19.1° in mineral oil), it could be theoretically increased, as silicone oil and mineral oil have refractive indices that are still relatively low (1.39 and 1.45 respectively).

Ethyl cinnamate was found to be less viscous than mineral oil and silicone oil [9]; relative to the other submersion fluids, the MEMS mirror in ethyl cinnamate reached larger output angles for the same corresponding input voltages, which resulted in an output angle vs. voltage curve that was more similar to that of open air. Out of the fluids tested, it had the highest refractive index of 1.56 [10], which meant the MEMS mirror could reach the largest maximum output angle (±20.4°) when it was at the limit of its mechanical tilt. Due to the increased refractive index of the submersion fluid, Snell's law

also took effect at much earlier stages during the mirror's actuation period, resulting in a nonlinear progression in the output angle vs. input voltage graphs, which allowed for reduced driving voltages during static angle testing.

B. Optical Analysis

During open-air testing of the MEMS mirror, it was observed that the laser spot remained relatively constant both in size and in shape. As shown in Fig 7, once the MEMS mirror was submerged in liquid, the laser spot became unfocused and more oblong as the output angle increased; while the mirror was reaching its mechanical tilting limit, the laser beam's angle of incidence approached the critical angle of the submersion fluid (a light ray's angle of incidence reaches the critical angle when the refracted light ray travels along the fluid-air boundary, resulting in an angle of refraction of 90°). This dramatically distorted the laser beam, which contributed to the laser spot's increased size and noncircular shape.

The laser spot's alteration in shape also prevented accurate measurements of its diameter, so future testing with photo detectors could provide a more precise analysis of the relationship between the elongation of the laser spot and the MEMS mirror's output angle. Further experiments also need to be completed to rectify the spot size issue and thereby facilitate the use of submerged MEMS mirrors in actual imaging technology.

C. Dynamic Testing Analysis

Due to the increased viscosity and thermal conductivity of the submersion fluids compared to air, significant dampening effects from the MEMS mirror's more restrictive environment increased the response time of the electrothermal actuators, preventing the mirror from fully tilting during high-speed operation.

The results obtained from dynamic testing indicated that lower frequency AC voltage (0.1-10.0 Hz) gave sufficient time for the MEMS mirror to tilt for its entire voltage range even when it was submerged in liquid. However, compared to open-air testing, significant reductions in the MEMS mirror's sweeping range occurred at much lower frequencies while the MEMS mirror was submerged, indicating that the viscosity and dampening effects of the fluids prevented the mirror from tilting to its full range while higher frequency AC voltage was applied.

Fig 8(c) showcases how ethyl cinnamate experienced the least amount of scanning range reduction due to its lower viscosity compared to silicone oil and mineral oil. Because the dampening effects were diminished, the MEMS mirror experienced less resistance while it was tilting, allowing it to preserve much more of its scanning range as the frequency was increased.

The higher thermal conductivity of the fluid environment prevented the electrothermal actuators from efficiently heating up, increasing the response time of the MEMS mirror; during high frequency testing, the mirror did not have enough time to fully tilt back and forth for its full range and eventually remained still once the frequency was further increased.

Dynamic testing also indicated that dampening effects from the submersion fluids prevented the submerged MEMS mirror from experiencing resonance at higher frequencies. In contrast, during open-air testing, once the mirror resonated, it could actuate at a much larger range (5.4°) and at very high frequencies (1422 Hz), as depicted in Fig 8(a).

Due to the submersion fluids' high thermal conductivity, viscosity, and dampening effects, submerged MEMS mirrors would be limited to slower scanning speeds. Along with that, they would not be able to take advantage of resonant scanning, which could further limit their effectiveness. However, for future testing, high RI submersion fluids with lower viscosities could reduce the resistance the mirror experiences and thus ameliorate the scanning speed issue.

For future tests, a logic analyzer should be used in conjunction with a photo detector to more accurately measure the displacement and movement of the laser spot as a function of the input AC voltage. Using this technique, comprehensive data regarding the response time of the MEMS mirror's electrothermal actuators could be collected and compared across the submersion fluids.

D. Final Conclusions

Submerging MEMS mirrors in fluids with high RI values increases the device's maximum output angle while still retaining fairly low driving voltages. However, due to the high thermal conductivity and dampening effects of such fluids, the submerged mirrors will no longer be able to perform resonant scanning and their scanning speeds may be limited to below 100 Hz. After experimentation with ethyl cinnamate, it has been deduced that submersion fluids with lower viscosities could be used to retain the scanning speed of the MEMS device. Optical tests also revealed that submersions fluids cause distortions in the laser beam; further testing will be required to rectify that issue for actual imaging applications.

Alternative submersion fluids with increased RI values also need to be tested. Other fields of research and technology require the use of such liquids; in UV lithography, the air gap between the final lens and the substrate can be replaced with a fluid, which increases the maximum resolution of the microcircuit by a factor of the fluid's RI value. In order to push the limits of this technology, many attempts have been made to increase the RI of the immersion fluid. One of the ways to do so is with the use of nanoparticles suspended in another medium, such as water or nonorganic oils, producing solutions with RI values close to 2. In UV lithography, the immersion fluid is engineered to have high transparency and low viscosity, which are both properties that aid with the MEMS mirror's performance [11].

A larger and more flexible scanning range would facilitate the use of MEMS-based endoscopic optical systems in medical devices; noninvasive surgeries can more be more easily performed with MEMS-based endoscopic devices that have increased scanning outputs. Medical practitioners would be privy to a new subset of information that could help treatment, such as cellular and molecular features, as well as images from deep tissue penetration. These technological and

scientific breakthroughs would enable more effective surgical procedures and diagnostic analyses.

Along with improved medical applications of MEMS devices, enhanced *in vivo* microscopy would be further enabled with the use of submersion fluids. MEMS mirrors, combined with optical fiber technology and remote illumination sources, can be used for confocal or two-photon microscopy on live, untethered specimen. With an improved scanning range, MEMS mirror-based probes would allow researchers to more accurately examine neural circuits and blood flow, opening greater opportunities for further neuroscience research.

Overall, the submersion approach has the potential to be a very successful yet simple way of producing a wide scanning MEMS device, which would enable new and more comprehensive imaging applications for endoscopic optical systems.

REFERENCES

[1] E. Pengwang, K. Rabenorosoa, M. Rakotondrabe, and N. Andreff, "Scanning Micromirror Platform Based on MEMS Technology for Medical Application," *Micromachines*, vol. 7, no. 2, p. 24, Jun. 2016.

[2] D. W. Piston, "Two-Photon Excitation Microscopy for Three-Dimensional Imaging of Living Intact Tissues," Fluorescence Microscopy, pp. 203–242, May 2017.

[3] L. Chen, "Fast High-resolution Miniature Two-photon Microscopy for Brain Imaging in Freely-behaving Mice at the Single-spine," *Optics in the Life Sciences Congress*, 2017.

[4] D. Wang, X. Zhang, L. Zhou, M. Liang, D. Zhang, and H. Xie, "An ultra-fast electrothermal micromirror with bimorph actuators made of copper/tungsten," *2017 International Conference on Optical MEMS and Nanophotonics (OMN)*, 2017.

[5] X. Zhang, L. Zhou, and H. Xie, "A Fast, Large-Stroke Electrothermal MEMS Mirror Based on Cu/W Bimorph," *Micromachines*, vol. 6, no. 12, pp. 1876–1889, Feb. 2015.

[6] X. Zhang, R. Zhang, S. Koppal, L. Butler, X. Cheng, and H. Xie, "MEMS mirrors submerged in liquid for wide-angle scanning," 2015 Transducers - 2015 18th International Conference on Solid-State Sensors, Actuators and Microsystems (TRANSDUCERS), 2015.

[7] Timms, R. (1985). Physical properties of oils and mixtures of oils. *Journal of the American Oil Chemists' Society*, 62(2), pp.241-249.

[8] Perrier, C. and Beroual, A. (2009). Experimental investigations on insulating liquids for power transformers: Mineral, ester, and silicone oils. *IEEE Electrical Insulation Magazine*, 25(6), pp.6-13.

[9] Katritzky, A., Chen, K., Wang, Y., Karelson, M., Lucic, B., Trinajstic, N., Suzuki, T. and Schüürmann, G. (2000). Prediction of liquid viscosity for organic compounds by a quantitative structure–property relationship. *Journal of Physical Organic Chemistry*, 13(1), pp.80-86.

[10] Wright, S., Zadrazil, I. and Markides, C. (2017). A review of solid–fluid selection options for optical-based measurements in single-phase liquid, two-phase liquid–liquid and multiphase solid–liquid flows. *Experiments in Fluids*, 58(9), p.108.

[11] Bremer, L., Tuinier, R., & Jahromi, S. (2009). High Refractive Index Nanocomposite Fluids for Immersion Lithography. *Langmuir, 25*(4), 12.